Hindawi Publishing Corporation
International Journal of Photoenergy
Volume 2012, Article ID 910256, 8 pages
doi:10.1155/2012/910256

Research Article

Simulation of Nonpolar p-GaN/i-$In_xGa_{1-x}N$/n-GaN Solar Cells

Ming-Jer Jeng

Department of Electronic Engineering and Green Technology Research Center, Chang-Gung University, 259 WenHwa 1st Road, Kweishan, Taoyuan 333, Taiwan

Correspondence should be addressed to Ming-Jer Jeng, mjjeng@mail.cgu.edu.tw

Received 1 November 2011; Revised 15 February 2012; Accepted 20 February 2012

Academic Editor: Peter Rupnowski

It is well known that nitride-based devices suffer the polarization effects. A promising way to overcome the polarization effects is growth in a direction perpendicular to the *c*-axis (nonpolar direction). Nonpolar devices do not suffer polarization charge, and then they have a chance to achieve the high solar efficiency. The understanding of the solar performance of non-polar InGaN-based solar cells will be interesting. For a pin non-polar solar cell with GaN p- and n-cladding layers, the conduction band offset (or barrier height, ΔE) between an intrinsic layer and n-GaN layer is an important issue correlating to the efficiency and fill factor. The efficiency and fill factor will be seriously degraded due to sufficiently high barrier height. To reduce a high barrier height, some graded layers with an energy bandgap between the energy bandgap of n-GaN and $In_xGa_{1-x}N$ intrinsic layer can be inserted to the interface of n-GaN and $In_xGa_{1-x}N$ layers. From simulation, it indicates that the insertion of graded layer is an effective method to lower energy barrier when there exists a high energy band offset in non-polar nitride devices.

1. Introduction

Nitride-based materials such as $In_xGa_{1-x}N$ have become important in fabricating photovoltaic devices due to their energy band gaps lying between 0.7 and 3.4 eV [1–5]. It can absorb the full solar spectrum by a single material of $In_xGa_{1-x}N$ with different indium contents. Many theoretical calculations on the performance evaluation of InGaN-based solar cells have been performed [1, 4, 5]. They demonstrated that a very high solar efficiency could be achieved. The direct bandgap properties and high absorption coefficients make it have great potential in photovoltaic application. Further, the GaN-based materials have a high resistant to high energy irradiation and temperature variations [6, 7]. Thus, it is suitable for space applications or high concentrator solar cell systems. However, a good-quality InGaN film with high indium composition cannot be obtained due to the low miscibility of InN in GaN. It also suffers polarization effects that degrade the device performance seriously [8–11]. Although the current nitride devices suffer the polarization effects, a promising way to overcome the polarization effects is growth in a direction perpendicular to the c-axis (nonpolar direction) [12–14]. In the heterojunction of p-GaN/i-$In_xGa_{1-x}N$/n-GaN structure on r-plane sapphire (nonpolar a-plane GaN), the nitride devices do not suffer polarization charge, and then they have a chance to achieve a high solar efficiency. The understanding of solar performance on non-polar InGaN-based solar cells will be interesting. In this work, the solar performance of non-polar p-GaN/i-$In_xGa_{1-x}N$/n-GaN solar cells with different $In_xGa_{1-x}N$ energy bandgaps from 1.1 to 3.2 eV has been simulated. It is observed that the conduction band offset between $In_xGa_{1-x}N$ and n-GaN layer will be an important issue for the efficiency of pin solar cells. Although a pn junction device is the most common structure in solar cells, a pin structure will be the best choice for high-defect materials due to drift field assistant properties. It is known that an intrinsic layer with low energy bandgap in pin solar cells has higher solar efficiency than that with high energy bandgap. But, one has to pay attention to the effects of the conduction band offset on the efficiency of solar cells. The photogenerated carriers cannot tunnel through the energy barrier if the ΔE is too high. To reduce the barrier height, some graded layers with an energy bandgap between the energy bandgap of n-GaN and $In_xGa_{1-x}N$ intrinsic layer can be inserted to the interface of n-GaN and $In_xGa_{1-x}N$ layers.

Table 1: The simulation parameters for $In_xGa_{1-x}N$ materials at 300 K [1].

Parameters	Expression	References
Energy bandgap (eV)	$E_g(In_xGa_{1-x}N) = 0.7x + 3.4(1-x) - 1.43x(1-x)$	[15]
Electron mobility ($cm^2\,eV^{-1}\,s^{-1}$)	Linear fitting: 170 at $P = 4 \times 10^{18}\,cm^{-3}$ and 100 at $P = 1 \times 10^{19}\,cm^{-3}$	[16, 17]
Hole mobility ($cm^2\,eV^{-1}\,s^{-1}$)	Linear fitting: 22 at $n = 3 \times 10^{17}\,cm^{-3}$ and 13 at $n = 1 \times 10^{18}\,cm^{-3}$	[16, 18]
Relative permittivity ε	$\varepsilon(In_xGa_{1-x}N) = x \cdot \varepsilon_{InN} + (1-x) \cdot \varepsilon_{GaN}$	[19, 20]
Electron affinity χ (eV)	$\chi_{GaN} + 0.7 \cdot (3.4 - E_g)$	[19, 21]
Effective density of states in the conduction band N_c (cm^{-3})	$N_c(In_xGa_{1-x}N) = xN_c^{InN} + (1-x)N_c^{GaN}$	[19]
Effective density of states in the valence band N_v (cm^{-3})	$N_v(In_xGa_{1-x}N) = xN_v^{InN} + (1-x)N_v^{GaN}$	[19]
Absorption coefficient α (cm^{-1})	$\alpha(\lambda) = 2.2 \times 10^5 \sqrt{(1.24/\lambda) - E_g}$	[19]
Carrier lifetime τ (ns)	1 ns	[22]
Surface recombination velocities S_{p0}, S_{pL}, S_{n0}, S_{nL} (cms^{-1})	1000	[23]

It can assist the photogenerated carriers to tunnel through the energy barrier and result in a higher solar efficiency. Thus, a graded GaN/$In_xGa_{1-x}N$/GaN solar cell grown on a nonpolar epilayer is simulated.

2. Simulation Parameters

The simulation parameters for $In_xGa_{1-x}N$ materials at 300 K are listed in Table 1 [1, 15–23]. The In composition dependence of $In_xGa_{1-x}N$ energy bandgap at 300 K is calculated by Wu's fitting equation [15]. The doping level dependence of the carrier mobility in $In_xGa_{1-x}N$ materials at 300 K is based on the fitting data [16–18], and the other related calculation parameters are assumed to be the same as GaN [22]. The simulation software of AMPS-1D is used to simulate the characteristics of $In_xGa_{1-x}N$ pin solar cells. The parameter of the front contact reflectivity is set to 0.1 in order to reflect general condition, and the back contact reflectivity is set to zero. It is noted that the series and shunt resistance of solar cells will degrade the solar performance. The series resistance mainly consists of contact and film resistance, and the shunt resistance results from the bulk and surface leakage current. It is known that the film quality of the p-type GaN is not good for a very high concentration. In addition, it is difficult to form a good ohmic contact when the concentration of the p-type GaN is lower than $1 \times 10^{17}\,cm^{-3}$. So, a concentration of $5 \times 10^{17}\,cm^{-3}$ is used as the doping concentration of p-type GaN region and a concentration of $1 \times 10^{18}\,cm^{-3}$ is assumed in the n-type GaN region. The concentration of the intrinsic layer is assumed as $5 \times 10^{16}\,cm^{-3}$ due to unintentionally high background concentration of donors. A quite good ohmic contact to p-GaN with a concentration of $5 \times 10^{17}\,cm^{-3}$ was obtained by semitransparent ohmic contact formation and metal grid deposition [3]. Thus, an ideal contact is assumed in this simulation. No attempt is made to find the optimum condition for the layer thickness and doping concentration. It just wants to demonstrate the needed layer structure of pin solar cells for a small energy bandgap of the intrinsic layer due to a high conduction band energy barrier at the interface of $In_xGa_{1-x}N$ and n-GaN layers.

3. Results and Discussions

Figures 1(a) and 1(b) show the efficiency and short circuit current (J_{sc}) as well as open circuit voltage (V_{oc}) and fill factor of $In_xGa_{1-x}N$ pn junction solar cells, respectively, with an In composition from $x = 0$ ($E_g = 3.4\,eV$) to $x = 0.75$ ($E_g = 1.11\,eV$) under AM1.5G illumination. The inset of Figures 1(a) and 1(b) shows the structure of $In_xGa_{1-x}N$ pn junction solar cells. By doing the simulation, the thickness of n-type region doped with $1 \times 10^{18}\,cm^{-3}$ is fixed at 250 nm and the thickness of p-type region doped with $5 \times 10^{17}\,cm^{-3}$ is optimized to obtain the highest efficiency at each In composition. A small optimum thickness range of 180 to 310 nm in p-type region is observed. It is noted that the efficiency reaches the maximum of 18.4% ($V_{oc} = 0.9\,V$, $J_{sc} = 26.1\,mA/cm^2$) at an In composition of $x = 0.6$ ($E_g = 1.44\,eV$) and then decreases with further increase in In composition. The higher the In composition of $In_xGa_{1-x}N$ is, the higher the J_{sc}, the lower the FF, and the lower the V_{oc} are. With the increase of In composition from $x = 0$ to 0.75, the V_{oc} linearly decreases from 2.64 to 0.59 V, the J_{sc} monotonously increases from 0.38 to 37.2 mA/cm^2, and the fill factor decreases from 0.89 to 0.72.

It is noted that a pn junction device has the best performance in solar cells for good-quality material. However, a pin structure will be the best choice for high-defect materials. In this paper, it is assumed that the carrier lifetime is 1 ns that is obtained from a more real quality GaN film [22]. So, the efficiency of the pn junction solar cells is better than that of the pin solar cells. One can demonstrate the clear advantages of the pin solar cells over pn junction if the carrier lifetime is shorter than 0.3 ns. (i.e., high-defect $In_{0.6}Ga_{0.4}N$ film) The carrier lifetime is strongly correlated to the film quality. The longer the carrier lifetime is, the better the film quality is. Figure 2 presents the comparison of the efficiency in $In_{0.6}Ga_{0.4}N$ pn and pin solar cells versus the carrier lifetime. Clearly, the pin solar cells exhibit better

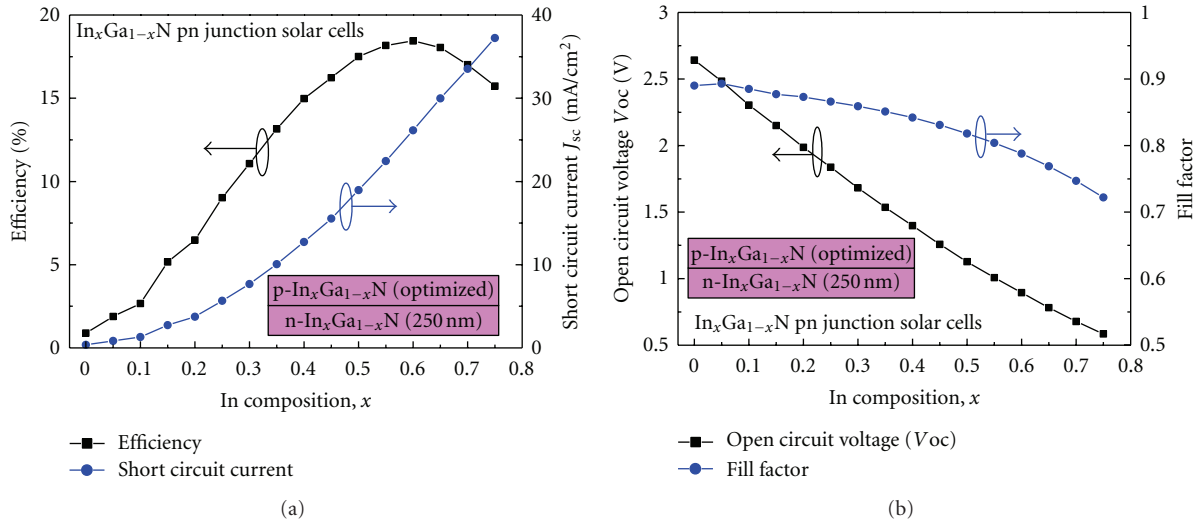

FIGURE 1: (a) The efficiency and short circuit current (J_{sc}) as well as (b) open circuit voltage (V_{oc}) and fill factor of $In_xGa_{1-x}N$ pn junction solar cells, respectively, with an In composition from $x = 0$ ($E_g = 3.4$ eV) to $x = 0.75$ ($E_g = 1.11$ eV) under AM1.5 illumination. The inset shows the structure of $In_xGa_{1-x}N$ pn junction solar cells.

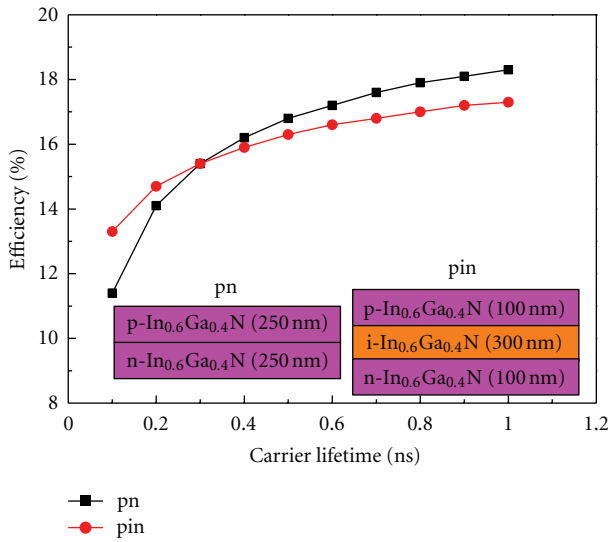

FIGURE 2: The efficiency of $In_{0.6}Ga_{0.4}N$ solar cells with a pn junction and a pin structure as a function of carrier lifetime.

efficiency than the pn solar cells when the carrier lifetime is shorter than 0.3 ns.

It is difficult to grow good-quality film especially in a thick $In_xGa_{1-x}N$ film with high In composition due to InN segregation problems. Presently, the film quality for a thin $In_xGa_{1-x}N$ film (several tenth nanometers) is good, but it is not good for a thick $In_xGa_{1-x}N$ film (several hundred nanometers). Generally, the acceptable film quality of $In_xGa_{1-x}N$ film is less than 100 nm for higher In composition ($x > 0.3$). However, the thickness of an $In_xGa_{1-x}N$ solar cell with enough light absorption is larger than 400 nm, which is mainly determined by the carrier lifetime and the material light absorption coefficients. The good solar cell performance of $In_xGa_{1-x}N$(p)/$In_xGa_{1-x}N$(n) or $In_xGa_{1-x}N$(p)/$In_xGa_{1-x}N$(i)/$In_xGa_{1-x}N$(n) structures with high In composition cannot be achieved due to poor $In_xGa_{1-x}N$ quality film with high In composition. An alternate structure of GaN(p)/$In_xGa_{1-x}N$(i)/GaN(n) is more easy to be achieved, like the recent published papers with relative high quantum efficiency [2, 3]. Thus, for more practical realization consideration, both of p-GaN and n-cladding layers are used in this simulation although the 17.3% efficiency of the $In_{0.6}Ga_{0.4}N$(p)/$In_{0.6}Ga_{0.4}N$(i)/$In_{0.6}Ga_{0.4}N$(n) solar cells is slightly better than the 16.8% efficiency of the GaN(p)/$In_{0.6}Ga_{0.4}N$(i)/GaN(n) with three graded-layer insertions at the carrier lifetime of 1 ns. The efficiency of p-GaN (100 nm)/i-$In_xGa_{1-x}N$ (200~500 nm)/n-GaN (100 nm) solar cells with an In composition of $x = 0.05$–0.3 is shown in Figure 3(a). Clearly, the higher the thickness of intrinsic layer, the higher the efficiency of the solar cell, but the increment is small due to high absorption in $In_xGa_{1-x}N$ layer. It is noted that the efficiency reaches the maximum of 9.2% at an In composition of $x = 0.26$ and then drops dramatically with the further increase of In composition. However, it is well known that an intrinsic layer with low energy bandgap in pin solar cells has higher solar efficiency than that with high energy bandgap under the same illumination. What reason causes the efficiency drop after the increase of In composition to higher than 0.26? It is possibly due to that a large conduction band energy barrier, ΔE, exists between $In_xGa_{1-x}N$ intrinsic layer and n-type GaN region. It is noted that high energy barrier in pin solar cells will seriously degrade the solar efficiency and the fill factor.

Figure 3(b) shows the fill factor of pin solar cells with various intrinsic layer thicknesses and In compositions. The fill factor begins to reduce dramatically when the In composition of $In_xGa_{1-x}N$ intrinsic layer is higher than

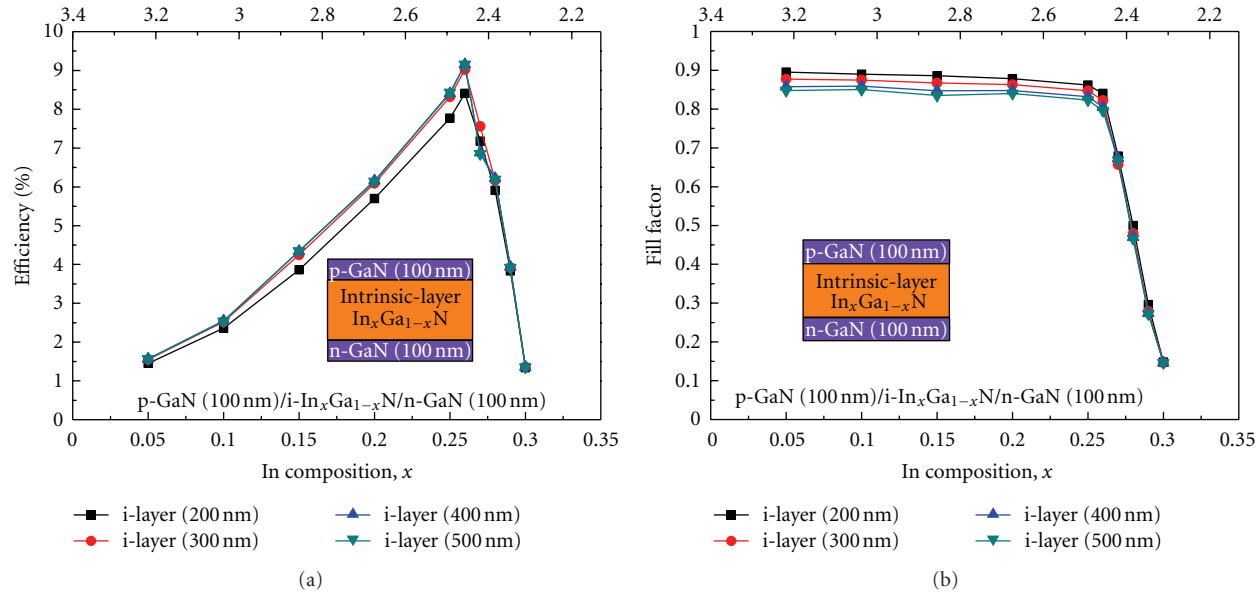

FIGURE 3: The efficiency (a) and the fill factor (b) of a p-GaN (100 nm)/i-$In_xGa_{1-x}N$ (200~500 nm)/n-GaN (100 nm) solar cells with an In composition of x = 0.05–0.3.

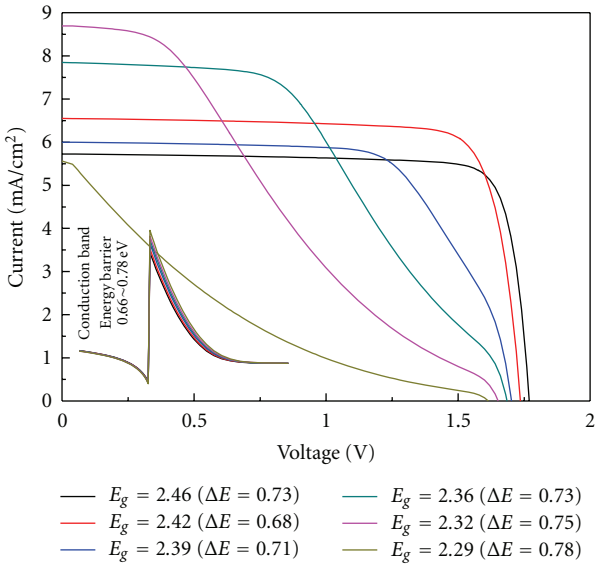

FIGURE 4: The current-voltage (I-V) curve of pin solar cells with various $In_xGa_{1-x}N$ energy bandgaps (corresponding to an In composition of 0.25–0.3 in Figure 2).

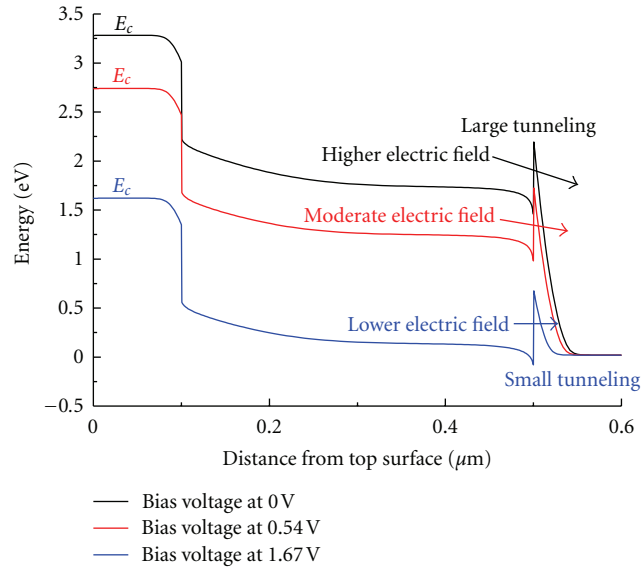

FIGURE 5: The conduction band energy diagram of $In_{0.3}Ga_{0.7}N$ pin solar cells at the voltage bias of 0, 0.54 and 1.67 V.

0.26, which is corresponding to an energy barrier of 0.68 eV. The photogenerated carriers cannot tunnel through the energy barrier if the ΔE is higher than 0.68 eV or if an existing electric field is small. It will seriously reduce the electric current and then result in a very low fill factor. It is noted that the diffusion current is dominated in the pn junction solar cells. However, the drift current is dominated in pin solar cells especially for high-defect materials. In the $In_xGa_{1-x}N$ pn junction structures, the diffusion current is dominated. In the $In_xGa_{1-x}N$(p)/$In_xGa_{1-x}N$(i)/$In_xGa_{1-x}N$(n) structures, the diffusion current is still dominated when the carrier lifetime is longer than 0.3 ns and the drift current will be dominated when the carrier lifetime is shorter than 0.3 ns (a lot of diffusion currents will be recombined by defects and cannot be effectively collected by the contact). In the GaN(p)/$In_xGa_{1-x}N$/GaN(n) structures, the drift current is dominated due to less current contribution in GaN, which generates less photocurrent by its high bandgap. More

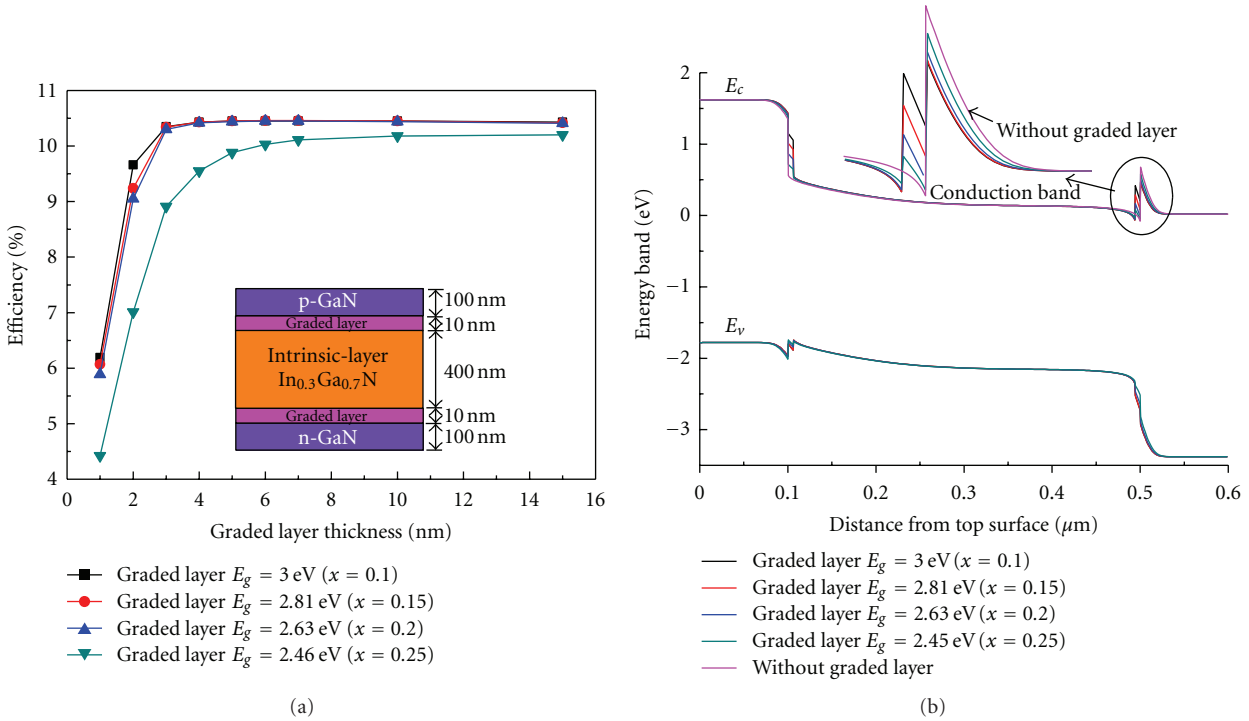

FIGURE 6: (a) The efficiency of one graded-layer $In_{0.3}Ga_{0.7}N$ pin solar cells with four different graded energy bandgap of 3.01, 2.81, 2.63, and 2.46 eV as a function of the graded layer thickness. (b) The energy band diagram of one graded-layer $In_{0.3}Ga_{0.7}N$ pin solar cells with four different graded energy bandgap of 3.01, 2.81, 2.63, and 2.46 eV.

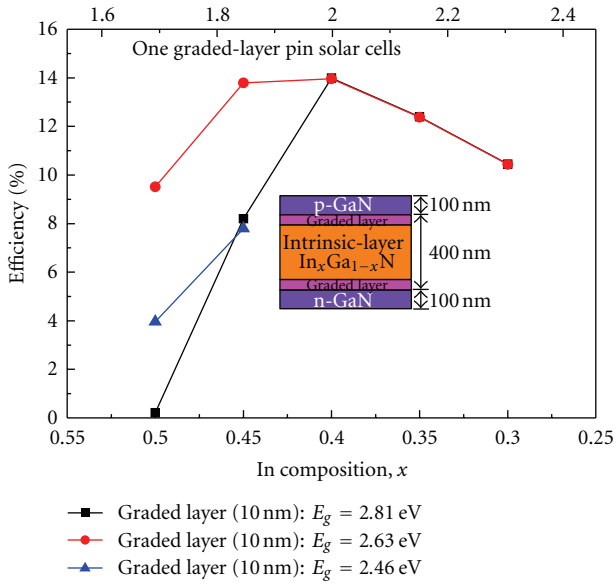

FIGURE 7: The efficiency of one graded-layer pin solar cells as a function of In composition from 0.3 to 0.5.

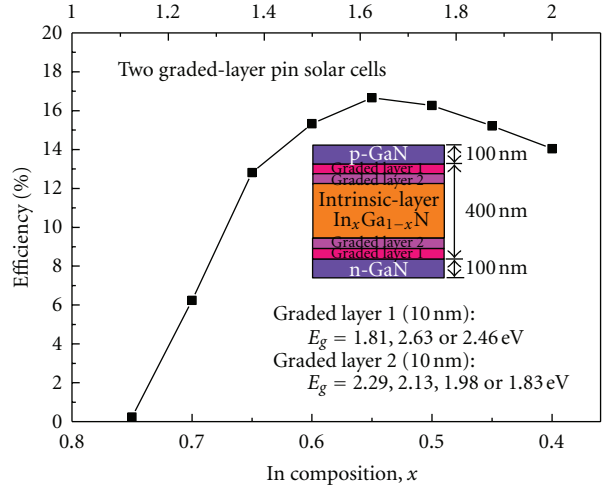

FIGURE 8: The efficiency of two graded-layer pin solar cells as a function of In composition from 0.4 to 0.75.

photogenerated currents will be contributed in GaN by the $In_xGa_{1-x}N$ intrinsic layer.

The current-voltage (I-V) curve of pin solar cells with various $In_xGa_{1-x}N$ energy bandgaps (corresponding to an In composition of 0.25–0.3 in Figure 3) is shown in Figure 4. Clearly, the I-V curve begins to deform with increase of voltage bias when the $In_xGa_{1-x}N$ energy bandgap is lower than 2.42 eV (x = 0.26). The deformation of I-V curve will gradually worsen with the decrease of $In_xGa_{1-x}N$ energy bandgap (increasing In composition). It means that the fill factor will become smaller. A completely deformed curve is observed in the $In_xGa_{1-x}N$ energy bandgap of 2.29 eV (x = 0.3), which has a very low fill factor of 0.13. The inset

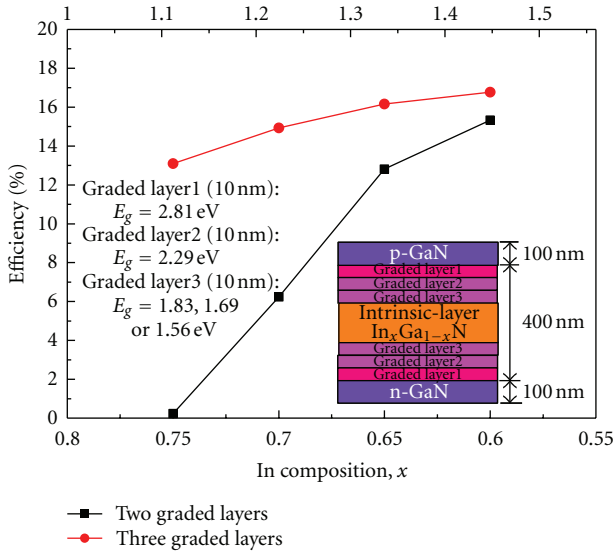

FIGURE 9: The efficiency of three graded-layer pin solar cells as a function of the In composition from 0.6 to 0.75.

of Figure 4 shows the conduction band energy barrier in pin solar cells with an In composition of 0.25–0.3. The $In_xGa_{1-x}N$ intrinsic layer with an In composition of 0.3 exhibits the highest energy barrier at the interface. Therefore, it has the lowest fill factor. Figure 5 shows the conduction band energy diagram of $In_{0.3}Ga_{0.7}N$ pin solar cells at the voltage bias of 0, 0.54 and 1.67 V, respectively. It can clearly explain why a large reduction of fill factor is in a high energy barrier of pin solar cells. At lower voltage bias (around 0V), there exists a high electric field in intrinsic layer. Most of the photogenerated carriers can tunnel through the energy barrier due to high field-assisted tunneling and then be collected by electrode contact; hence, a high J_{sc} is observed. However, the electric field will gradually reduce with the increase of voltage bias. At a higher voltage bias, most of the photogenerated carriers cannot tunnel through the energy barrier due to low field-assisted tunneling or high energy barriers, existing at the interface between $In_xGa_{1-x}N$ intrinsic layer and n-GaN region. Few photogenerated carriers are collected in the electrode contact and result in a small electric current. It is noted that a reduction of the electric current will begin to occur at moderate voltage bias if the energy barrier at the interface is too high, for example, in the case of In composition with 0.27–0.3 it will seriously degrade the fill factor of solar cells due to poor current shape gradually changing from a seemingly rectangular shape to a triangular shape with an increasing energy barrier, which is consistent with the *I-V* observations in Figure 4. Recently, both $In_{0.2}Ga_{0.8}N$/GaN and $In_{0.28}Ga_{0.72}N$/GaN multiple quantum well solar cells (MQWSCs) are experimentally fabricated and compared. The *I-V* curve behavior of $In_{0.2}Ga_{0.8}N$/GaN and $In_{0.28}Ga_{0.72}N$/GaN MQWSCs is similar to the simulation observation in Figure 4 [24]. The higher the energy barrier height is, the lower the fill factor is. The $In_{0.28}Ga_{0.72}N$/GaN MQWSCs with the higher energy barrier between well and barrier materials exhibit more deformed *I-V* curve and lower fill factor than the $In_{0.2}Ga_{0.8}N$/GaN MQWSCs. It is believed that this behavior is possibly related to the energy barrier height (or conduction band offset).

To reduce the high energy barrier height, one can insert a graded layer of 10 nm with an energy bandgap between the energy bandgap of GaN and $In_xGa_{1-x}N$ intrinsic layer to the interface of GaN and $In_xGa_{1-x}N$. Figure 6(a) presents the efficiency of one graded-layer $In_{0.3}Ga_{0.7}N$ pin solar cells with four different graded energy bandgaps of 3.01, 2.81, 2.63, and 2.46 eV as a function of the graded layer thickness. The pin solar cells with a graded layer having an energy bandgap of 2.81 eV exhibit the highest efficiency, when the energy barrier is closely to a half of bandgap difference between GaN (3.4 eV) and $In_{0.3}Ga_{0.7}N$ (2.29 eV). A graded layer with an energy bandgap of 2.46 eV has the worst efficiency due to poor fill factor (large energy barrier). To achieve high efficiency, the optimized thickness of the graded layer is observed at 6 nm and the efficiency drops dramatically at 2 nm. The energy band diagram of one graded-layer $In_{0.3}Ga_{0.7}N$ pin solar cells with four different graded energy bandgap of 3.01, 2.81, 2.63, and 2.46 eV is shown in Figure 6(b). Clearly, an $In_{0.3}Ga_{0.7}N$ pin solar cell with a graded-layer insertion exhibits an energy barrier lower than that without a graded layer insertion. Especially for a graded layer with an energy bandgap of 2.81 eV, it has the lowest energy barrier. This indicates that the barrier height (ΔE) between an intrinsic layer and n-GaN is an important issue correlating to the efficiency and fill factor. The higher the barrier height is, the poorer the efficiency and fill factor are, as shown in Figure 4.

As mentioned above, it is known that the efficiency and fill factor will seriously degrade when an In composition of $In_xGa_{1-x}N$ intrinsic layer is larger than 0.26. In order to improve the solar efficiency, a graded layer is needed to lower the energy barrier height. Figure 7 shows the efficiency of one graded-layer pin solar cells as a function of In composition from 0.3 to 0.5. The efficiency of $In_{0.3}Ga_{0.7}N$ pin solar cells can be improved from 1.4% (as shown in Figure 3(a)) to 10.5% with a graded-layer insertion due to a great improvement of the fill factor from 0.15 to 0.87 (due to a lower barrier height ΔE). It is interesting to note that one graded-layer insertion has an effective improvement of efficiency only in the In composition range of 0.3–0.45. The efficiency begins to drop when an In composition of $In_xGa_{1-x}N$ intrinsic layer is larger than 0.45. The graded layer with an In composition of 0.2 has better efficiency than those with the In composition of 0.15 or 0.25 in higher In composition of $In_xGa_{1-x}N$ intrinsic layer ($x = 0.4$ or 0.45). One simple rule that can be used to determine the In composition of a graded layer is a half value of In composition of $In_xGa_{1-x}N$ intrinsic layer. For example, a pin solar cell with an In composition of 0.3 in $In_xGa_{1-x}N$ intrinsic layer optimally needs a graded layer with an In composition of 0.15, while that with an In composition of 0.4 or 0.45 needs a graded layer with an In composition of 0.2. In addition, the energy barrier height of $In_xGa_{1-x}N$ pin solar cells with an In composition of 0.5 is still too high and results in a poor efficiency although a graded layer has been inserted. That is to say, more graded layers are needed for high In composition $In_xGa_{1-x}N$ intrinsic layer ($x > 0.45$).

Table 2: The optimum In-composited combination of two graded layers for each In composition of $In_xGa_{1-x}N$ pin solar cells.

The In composition of $In_xGa_{1-x}N$ intrinsic layer (corresponding energy bandgap eV)	0.4 (1.98)	0.45 (1.83)	0.5 (1.69)	0.55 (1.56)	0.6 (1.44)	0.65 (1.32)	0.7 (1.21)	0.75 (1.11)
The In composition of the 1st graded layer	0.15 (2.81)	0.15 (2.81)	0.15 (2.81)	0.15 (2.81)	0.2 (2.63)	0.2 (2.63)	0.2 (2.63)	0.25 (2.46)
The In composition of the 2nd graded layer	0.3 (2.29)	0.3 (2.29)	0.3 (2.29)	0.35 (2.13)	0.4 (1.98)	0.4 (1.98)	0.45 (1.83)	0.5 (1.69)

Table 3: The optimum In-composited combination of three graded layers for each In composition of $In_xGa_{1-x}N$ pin solar cells.

The In composition of $In_xGa_{1-x}N$ intrinsic layer (corresponding energy bandgap eV)	0.6 (1.44)	0.65 (1.32)	0.7 (1.21)	0.75 (1.11)
The In composition of the 1st graded layer	0.15 (2.81)	0.15 (2.81)	0.15 (2.81)	0.15 (2.81)
The In composition of the 2nd graded layer	0.3 (2.29)	0.3 (2.29)	0.3 (2.29)	0.35 (2.13)
The In composition of the 3rd graded layer	0.45 (1.83)	0.5 (1.69)	0.5 (1.69)	0.55 (1.56)

The efficiency of two graded-layer pin solar cells as a function of In composition from 0.4 to 0.75 is shown in Figure 8. Clearly, an $In_{0.6}Ga_{0.4}N$ pin solar cell with two graded-layer insertion exhibits the highest efficiency of 15.3%. The efficiency of $In_xGa_{1-x}N$ pin solar cells dramatically drops when an In composition of pin solar cell is at 0.75. It means that three graded-layer insertions are needed to lower the energy barrier height in such high In composition. Table 2 lists the optimum In composite combination of two graded layers for each In composition of $In_xGa_{1-x}N$ pin solar cells. An equally spacing interval of In composition is observed to achieve high efficiency. It is reasonable due to that it can equally minimize the energy barrier height.

Figure 9 shows the efficiency of three graded-layer pin solar cells as a function of the In composition from 0.6 to 0.75. The efficiency of two graded-layer pin solar cells is also shown for comparison. A great improvement of efficiency from 0.23% to 13.1% can be seen at an In composition of 0.75 by three graded-layer insertion. The three graded-layer pin solar cells exhibits a little increase of efficiency at an In composition lower than 0.7 in comparison with two graded-layer pin solar cells. The $In_{0.6}Ga_{0.4}N$ pin solar cells with three graded-layer insertions exhibit the highest efficiency of 16.8% ($V_{oc} = 0.83$ V and $J_{sc} = 26.2$ mA/cm^2). The optimum In composite combination of three graded layers for each In composition of $In_xGa_{1-x}N$ pin solar cells is listed in Table 3. For the In composition range of 0.6 to 0.75, the first graded layer with an In composition of 0.15 and the second graded layer with an In composition of 0.3 or 0.35 are the best choices. The selection rule of In composition of the third graded layer is that the In composition differences are no more than 0.2 between $In_xGa_{1-x}N$ intrinsic layer and the second graded layer.

4. Conclusions

The non-polar $In_xGa_{1-x}N$ pn and pin junction solar cells with different In compositions have been simulated. It is observed that an $In_{0.6}Ga_{0.4}N$ ($E_g = 1.44$ eV) pn junction solar cell exhibits the highest efficiency of 18.4% ($V_{oc} = 0.9$ V and $J_{sc} = 26.1$ mA/cm^2). For the pin solar cells with a GaN/$In_xGa_{1-x}N$/GaN structure, a graded layer is needed at the interface of $In_xGa_{1-x}N$ intrinsic layer and n-GaN region when the energy barrier height is too high. In order to obtain higher efficiency, one graded layer is necessary when the In composition of $In_xGa_{1-x}N$ intrinsic layer is larger than 0.26, while two graded layers are necessary when the In composition of $In_xGa_{1-x}N$ intrinsic layer is larger than 0.45. Finally, three graded layers are needed when the In composition of $In_xGa_{1-x}N$ intrinsic layer is larger than 0.7. It is interesting to note that one graded-layer insertion has an effective improvement of efficiency only in the In composition range of 0.3–0.45. Two and three graded-layer insertions are needed to improve the efficiency and fill factor when the In composition of the intrinsic layer is larger than 0.45 and 0.7, respectively. The GaN/$In_{0.6}Ga_{0.4}N$/GaN pin solar cells with two and three graded-layer insertions exhibit the highest efficiency of 15.3% and 16.8%, respectively ($V_{oc} = 0.82$ V and $J_{sc} = 26.2$ mA/cm^2). This simulation work indicates that the insertion of graded layer is an effective method to lower energy barrier when there exists a high energy band offset in non-polar nitride devices.

Acknowledgments

This work was supported by the National Science Council of Taiwan, (Project no. NSC98-2221-E-182-006). The author acknowledges the use of AMPS-1D developed by Professor Fonash of the Pennsylvania State University.

References

[1] X. Zhang, X. Wang, H. Xiao et al., "Simulation of In0.65Ga0.35 N single-junction solar cell," *Journal of Physics D*, vol. 40, no. 23, pp. 7335–7338, 2007.

[2] O. Jani, I. Ferguson, C. Honsberg, and S. Kurtz, "Design and characterization of GaNInGaN solar cells," *Applied Physics Letters*, vol. 91, no. 13, Article ID 132117, 2007.

[3] C. J. Neufeld, N. G. Toledo, S. C. Cruz, M. Iza, S. P. DenBaars, and U. K. Mishra, "High quantum efficiency InGaN/GaN solar cells with 2.95 eV band gap," *Applied Physics Letters*, vol. 93, no. 14, Article ID 143502, 2008.

[4] H. Hamzaoui, A. S. Bouazzi, and B. Rezig, "Theoretical possibilities of InxGa1-xN tandem PV structures," *Solar Energy Materials and Solar Cells*, vol. 87, no. 1–4, pp. 595–603, 2005.

[5] O. Jani, C. Honsberg, A. Asghar et al., "Characterization and analysis of InGaN photovoltaic devices," in *Proceedings of the 31st IEEE Photovoltaic Specialists Conference*, pp. 37–42, Lake Buena Vista, Fla, USA, January 2005.

[6] J. F. Muth, J. H. Lee, I. K. Shmagin et al., "Absorption coefficient, energy gap, exciton binding energy, and recombination lifetime of GaN obtained from transmission measurements," *Applied Physics Letters*, vol. 71, no. 18, pp. 2572–2574, 1997.

[7] J. Wu, W. Walukiewicz, K. M. Yu et al., "Superior radiation resistance of $In_{1-x}Ga_xN$ alloys: full-solar-spectrum photovoltaic material system," *Journal of Applied Physics*, vol. 94, no. 10, pp. 6477–6482, 2003.

[8] M. Mehta, O. Jani, C. Honsberg, B. Jampana, I. Ferguson, and A Doolittle, "Modifying PC1D to model spontaneous and piezoelectric polarization in III-V nitride solar cells," in *Proceedings of the 22nd European Photovoltaic Solar Energy Conference*, p. 409, Milan, Italy, 2007.

[9] O. Jani, B. Jampana, and M. Mehta, "Optimization of GaN window layer for InGaN solar cells using polarization effect," in *Proceedings of the 33rd IEEE Photovoltaic Specialists Conference*, pp. 1–4, San Diego, Calif, USA, May 2008.

[10] M. J. Jeng, "Influence of Polarization on the Efficiency of $In_xGa_{1-x}N$/GaN p–i–n Solar Cells," *Japanese Journal of Applied Physics*, vol. 49, Article ID 128001, 2 pages, 2010.

[11] Z. Q. Li, M. Lestradet, Y. G. Xiao, and S. Li, "Effects of polarization charge on the photovoltaic properties of InGaN solar cells," *Physica Status Solidi A*, vol. 208, no. 4, pp. 928–931, 2011.

[12] C. Q. Chen, M. E. Gaevski, W. H. Sun et al., "GaN homoepitaxy on freestanding $(1\bar{1}00)$ oriented GaN substrates," *Applied Physics Letters*, vol. 81, no. 17, pp. 3194–3196, 2002.

[13] H. M. Ng, "Molecular-beam epitaxy of GaN/$Al_xGa_{1-x}N$ multiple quantum wells on R-plane $(10\bar{1}2)$ sapphire substrates," *Applied Physics Letters*, vol. 80, no. 23, pp. 4369–4371, 2002.

[14] A. Chitnis, C. Chen, V. Adivarahan et al., "Visible light-emitting diodes using a-plane GaN-InGaN multiple quantum wells over r-plane sapphire," *Applied Physics Letters*, vol. 84, no. 18, pp. 3663–3665, 2004.

[15] J. Wu, W. Walukiewicz, K. M. Yu et al., "Small band gap bowing in In1-xGaxN alloys," *Applied Physics Letters*, vol. 80, no. 25, p. 4741, 2002.

[16] K. Kumakura, T. Makimoto, N. Kobayashi, T. Hashizume, T. Fukui, and H. Hasegawa, "Minority carrier diffusion length in GaN: dislocation density and doping concentration dependence," *Applied Physics Letters*, vol. 86, no. 5, Article ID 052105, pp. 1–3, 2005.

[17] P. Kozodoy, H. Xing, S. P. DenBaars et al., "Heavy doping effects in Mg-doped GaN," *Journal of Applied Physics*, vol. 87, no. 4, pp. 1832–1835, 2000.

[18] H. M. Ng, D. Doppalapudi, T. D. Moustakas, N. G. Weimann, and L. F. Eastman, "The role of dislocation scattering in n-type GaN films," *Applied Physics Letters*, vol. 73, no. 6, pp. 821–823, 1998.

[19] M. E. Levinshtein, S. L. Rumyantsev, and M. S. Shu, *Properties of Advanced Semiconductor Materials*, John Wiley & Sons, New York, NY, USA, 2001.

[20] A. S. Barker and M. Ilegems, "Infrared lattice vibrations and free-electron dispersion in GaN," *Physical Review B*, vol. 7, no. 2, pp. 743–750, 1973.

[21] N. Li, *Simulation and analysis of GaN-based photoelectronic devices*, Dissertation, Institute of Semiconductor, Chinese Academy of Sciences, Beijing, China, 2005.

[22] G. F. Brown, J. W. Ager, W. Walukiewicz, and J. Wu, "Finite element simulations of compositionally graded InGaN solar cells," *Solar Energy Materials and Solar Cells*, vol. 94, no. 3, pp. 478–483, 2010.

[23] R. Aleksiejunas, M. Sudzius, V. Gudelis et al., "Carrier transport and recombination in InGaN/GaN heterostructures, studied by optical four-wave mixing technique," *Physica Status Solidi*, vol. 0, no. 7, pp. 2686–2690, 2003.

[24] M.-J. Jeng, Y.-L. Lee, and L.-B. Chang, "Temperature dependences of $In_xGa_{1-x}N$ multiple quantum well solar cells," *Journal of Physics D*, vol. 42, no. 10, Article ID 105101, 2009.